



ORIGINAL ARTICLE

Synthesis, *in vitro* evaluation, and molecular docking studies of benzofuran based hydrazone a new inhibitors of urease



Jana Abdullah Al-Mohammadi ^{a,b}, Muhammad Taha ^{b,*}, Fazal Rahim ^c,
Rafaqat Hussain ^c, Hanan aldossary ^b, Rai Khalid Farooq ^d, Abdul Wadood ^e,
Muhammad Nawaz ^f, Mohammed Salahuddin ^b, Khalid Mohammed Khan ^g,
Nizam Uddin ^h

^a Mawhiba Research Enrichment Program-2021, King Abdulaziz and His Companions Foundation for Giftedness and Creativity, Riyadh, Saudi Arabia

^b Department of Clinical Pharmacy, Institute for Research and Medical Consultations (IRMC), Imam Abdulrahman Bin Faisal University, P.O. Box 1982, Dammam 31441, Saudi Arabia

^c Department of Chemistry, Hazara University, Mansehra 21300, Khyber Pakhtunkhwa, Pakistan

^d Department of Neuroscience Research, Institute for Research and Medical Consultations (IRMC), Imam Abdulrahman Bin Faisal University, P.O. Box 1982, Dammam 31441, Saudi Arabia

^e Department of Biochemistry, Abdul Wali Khan University Mardan, Mardan 23200, Pakistan

^f Department of Nano-Medicine Research, Institute for Research and Medical Consultations (IRMC), Imam Abdulrahman Bin Faisal University, P.O. Box 1982, Dammam 31441, Saudi Arabia

^g H. E. J. Research Institute of Chemistry, International Center for Chemical and Biological Sciences, University of Karachi, Karachi 75270, Pakistan

^h Department of Chemistry, University of Karachi, Karachi 75270, Pakistan

Received 13 January 2022; accepted 6 May 2022

Available online 11 May 2022

KEYWORDS

Synthesis;
Urease;
Benzofuran;
Hydrazone;
Structure activity relationship;
Molecular docking

Abstract This work has described the synthesis of novel class (1–25) of benzofuran based hydrazone. The hybrid scaffolds (1–25) of benzofuran based hydrazone were evaluated *in vitro*, for their urease inhibition. All the newly synthesized analogues (1–25) were found to illustrate moderate to good urease inhibitory profile ranging from 0.20 ± 0.01 to 36.20 ± 0.70 μM . Among the series, compounds **22** ($\text{IC}_{50} = 0.20 \pm 0.01$ μM), **5** ($\text{IC}_{50} = 0.90 \pm 0.01$ μM), **23** ($\text{IC}_{50} = 1.10 \pm 0.01$ μM) and **25** ($\text{IC}_{50} = 1.60 \pm 0.01$ μM) were found to be the many folds more potent than thiourea as standard inhibitor ($\text{IC}_{50} = 21.86 \pm 0.40$ μM). The elevated inhibitory profile of these analogues

* Corresponding author.

Peer review under responsibility of King Saud University.



Production and hosting by Elsevier

might be due to presence of dihydroxy and fluoro groups at different position of phenyl ring **B** attached to hydrazone skeleton. These dihydroxy and fluoro groups bearing compounds have shown many folds better inhibitory profile through involvement of oxygen of dihydroxy groups in hydrogen bonding with active site of enzymes. Various types of spectroscopic techniques such as ^1H -, ^{13}C - NMR and HREI-MS spectroscopy were used to confirm the structure of all the newly developed compounds. To find SAR, molecular docking studies were performed to understand, the binding mode of potent inhibitors with active site of enzymes and results supported the experimental data.

© 2022 The Author(s). Published by Elsevier B.V. on behalf of King Saud University. This is an open access article under the CC BY-NC-ND license (<http://creativecommons.org/licenses/by-nc-nd/4.0/>).

1. Introduction

Urease (E.C 3.5.1.5) plays an important role in the virulence of some bacterial pathogens as well as determinant in pathogenesis of many diseases in human. It is involved in the production of infectious stones; add to the pathogenesis of urolithiasis, pyelonephritis, and hepatic encephalopathy (Weatherburn, 1967). It was reported by the facts that numerous gastro duodenal disorder such as gastric cancer, encrustation of urinary catheter, peptic ulcer and duodenal ulcer were caused by *Helicobacter pylori*. The survival of *Helicobacter pylori* was paved by increase of pH in aqueous medium through liberation of amount of ammonia (Devesa et al., 1998). Additionally, urease causes kidney stones formation but also engages in the growth of urolithiasis, pyelonephritis, and hepatic encephalopathy (Martelli et al., 1981). In agriculture, during urea fertilization, high urease activity results in significant environmental and economic losses by discharge of abnormally huge amounts of ammonia in atmosphere. This also leads to plant damage by depriving them from essential nutrients, secondary ammonia toxicity and increase in pH of the soil (Mobley & Hausinger, 1989). In humans to control destructive effects caused by ureolytic bacterial infection, urease inhibitors play very key role to prevent degradation of urea. Inhibition of enzyme through synthesis of organic inhibitors have attracted the attention of medicinal chemists as an important and valuable tool in discovery of drugs leading to designing and development of biologically more active drugs (Saify et al., 2014). Variety of organic compounds such as hydroxamate complex, homoserine lactone derivative, thiophosphoric triamides, oxadiazoles derivatives, thiourea, ethyl 4-(3-benzothioureido) benzoates derivatives, oxindole derivatives and thiobarbituric acid derivatives have been used over the past few decades for the inhibition of urease (Akhtar et al., 2014; Cheng et al., 2014; Czerwonka et al., 2014; Khan et al., 2014a; 2014b; Ludden et al., 2000; Saeed et al., 2014; Taha et al., 2015). In addition, numerous anti-urease agents were reported and gained much attention of medicinal chemists through inhibition of urease enzyme (Font et al., 2008) (see Table 1).

Benzofuran motif bearing scaffolds based on its physiological properties, dynamic nature and their profound chemotherapeutic during last few decades got much attentions to medicinal chemists due to its versatile nature and functions as key entity in designing and synthesis of pharmacologically

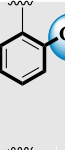
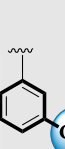
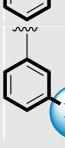
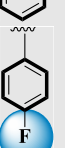
and therapeutically more potentials drugs. Benzofuran and its scaffolds are known to possess the biological activities of interest such as such as antimicrobial (Alper-Hayta et al., 2008; M. W. Khan et al., 2005), anticancer (Asoh et al., 2009; Mahboobi et al., 2007), anti-inflammatory (Jadhav et al., 2008), anticholinesterase (Belluti et al., 2005; Luo et al., 2005) and antihistaminergic (Coward et al., 2005; Gfesser et al., 2005; Peschke et al., 2006). Apart from these, benzofuran skeleton bearing scaffolds also finds applications as fluorescent sensor (Karatas et al., 2006), oxidant (Oter et al., 2007), antioxidant, brightening agent and in the field of agriculture (Habermann et al., 1999). Benzo[b]furan skeleton based pharmacophore were extensively employed in numerous clinical drugs including amiodarone hydrochloride (a cardio-vascular) and fruquintinib (an anti-tumor) (Cao et al., 2016; Flynn et al., 2011). Furthermore, some inhibitors (**1–4**) of tubulin polymerization also exhibit the benzo[b] furan pharmacophore (Fig. 2) (Flynn et al., 2002; Romagnoli et al., 2008) which emerged to bind to the colchicines binding domain of tubulin and Therefore, the benzo[b]furan-2-carboxylic acid as well as shikonin were united, and in order to attain the excellent compounds (see Figs. 3-5).

Hydrazone motif bearing analogues were found to have numerous pharmacological and biological profile such as anti-inflammatory, antimicrobial, antifungal, analgesic, antiviral, anti-tubercular, anticancer, antimalarial, antiplatelet, cardio protective, anticonvulsant, anti-trypanosomal, antihelminthic, antischistosomiasis and antiprotozoal (Rollas and Küçükgülzel, 2007; Narang et al., 2012; Negi et al., 2012) (Scheme 1).

The heterocyclic entity bearing scaffolds have gained substantial attention to medicinal chemists owing to their interesting and versatile chemical profile. Therefore, in search of lead molecules, our research group had reported numerous biologically interesting heterocyclic moieties of different classes to explore their inhibitory potentials. In recent past, we had developed an approach for the synthesis of nitrogen and oxygen bearing heterocyclic scaffolds as promising inhibitors of urease (Rahim et al., 2015).

Encouraged by the success of nitrogen and oxygen bearing heterocyclic scaffolds as promising inhibitors of urease, thymidine phosphorylase, α -glucosidase and α -amylase, we sought to further expand the scope and diversity of this practical approach by developing an approach for the synthesis of

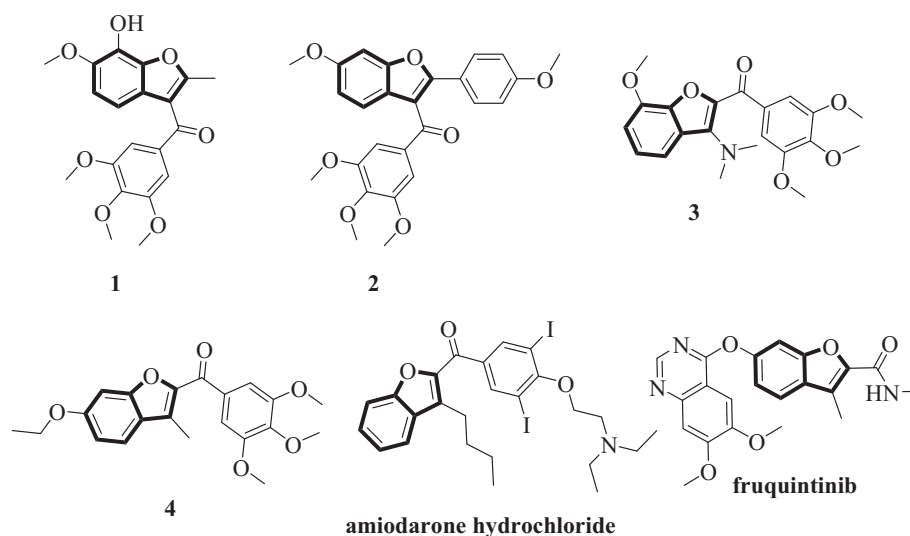
Table 1 *In vitro* urease inhibitory activities of benzofuran based hydrazone derivatives (1–25).

S.NO	Ring B	IC ₅₀ ± SEM ^a [μM]	S.NO	Ring B	IC ₅₀ ± SEM ^a [μM]
1		17.60 ± 0.30	14		23.90 ± 0.50
2		1.90 ± 0.10	15		36.20 ± 0.70
3		2.10 ± 0.10	16		28.20 ± 0.50
4		26.60 ± 0.50	17		22.20 ± 0.50
5		0.90 ± 0.01	18		3.80 ± 0.10
6		6.70 ± 0.20	19		34.90 ± 0.70
7		18.90 ± 0.40	20		2.70 ± 0.10
8		1.70 ± 0.10	21		N.A.
9		31.10 ± 0.30	22		0.20 ± 0.01
10		19.30 ± 0.40	23		1.10 ± 0.01
11		32.20 ± 0.30	24		3.80 ± 0.10
12		14.60 ± 0.30	25		1.60 ± 0.01

(continued on next page)

Table 1 (continued)

S.NO	Ring B	IC ₅₀ ± SEM ^a [μM]	S.NO	Ring B	IC ₅₀ ± SEM ^a [μM]
13		9.70 ± 0.20	–	–	–
Standard Thiourea					21.86 ± 0.40

**Fig. 1** Structure of tubulin assembly inhibitors.

benzofuran based hydrazone (**1–25**) scaffolds with the hope that it might show better inhibitory potentials against *urease* enzyme.

2. Results and discussion

2.1. Chemistry

In the first step, benzofuran (**a**) in ethanol and hydrazine hydrate mixture (50 mL:1) was added. The reaction mixture was placed over pre-heated sand bath and stirred under condition of reflux for about 3hrs to afford formation of benzofuran based hydrazone as an intermediate (**b**). In the next step, an intermediate (**b**) was added to solution of corresponding benzaldehyde in methanol along with few drops of glacial acetic acid and the resulting residue put on stirring under reflux until the consumption of substrate (**b**) was completed (the progress of the reaction was monitored by TLC). The solvent was evaporated and resulting solid residue was dried and washing with n-hexane to afford the synthesis of desired benzofuran based hydrazone scaffolds (**c**) (**1–25**) in excellent yield. All synthetic benzoxazole based hydrazone were fully characterized by different spectroscopic techniques including ¹H and ¹³C NMR spectroscopy.

The ¹H NMR spectrum of compound (**3**) was recorded in DMSO-*d*₆ on a Bruker 600 MHz instrument. The peak for hydrogen attached to nitrogen was observed at δ_H 12.36 (s, 1H, –NH). The most downfield singlets of two –OH protons

linked to benzene ring were resonated at δ_H 10.71 and 10.03, respectively. The molecule comprises of benzofuran ring with **5** protons and an aryl ring having **3** protons. Among benzofuran ring protons, signal for (**H-2**) was appeared at δ_H 8.72 as singlet, while (**H-4**) and (**H-5**) were resonated at δ_H 7.81 (d, *J*_(4/5) = 7.6 Hz, 1H, H-4) and 7.66 (d, *J*_(5/4) = 7.6 Hz, 1H, H-5) as doublets, respectively. However, (**H-6**) and (**H-7**) were resonated at 7.55 (t, *J*_(6/4, 5) = 9.2 Hz, 1H, H-6) and 7.54 (d, *J*_(7/6) = 6.5 Hz, 1H, H-7) as triplet and doublet respectively. **Proton-6** showing coupling with **protons 4** and **5** on both side to give triplet having coupling constant 9.2 Hz. The singlet at δ_H 8.32 was observed for HC = N. On the other hand, three distinct peaks were shown for aryl ring protons labeled as (**H-2'**), (**H-4'**) and (**H-6'**). Among them, triplet for (**H-6'**) was observed at δ_H 7.40 showing coupling *meta*-coupling with **H-4'** and **H-2'** on both side with coupling constant 1.8 Hz. Furthermore, the (**H-2'**) and (**H-4'**) were resonated at δ_H 7.09 (d, *J*_(2', 4') = 2.0 Hz, 1H, H-2') and δ_H 6.93 (dd, *J*_(4', 2') = 2.4 Hz, *J*_(4', 6') = 2.8 Hz, 1H, H-4') as doublet and doublet of doublet.

As for compound **3**, the ¹³C NMR signals δ_{C-13} at 162.6 was attributed to carbonyl carbon (C = O), while two peaks at δ_{C-13} 160.3 (C–OH) and 160.3 (C–OH) were observed for benzene ring carbons holding hydroxy groups. The signal for other four carbons of benzene ring were appeared at δ_{C-13} 136.8 (C), 107.8 (CH), 107.8 (CH) and 106.2 (CH) respectively. The bridged carbons of benzofuran were resonated at δ_{C-13} 155.7 (C) and 122.7 (C) respectively. The peaks corresponding

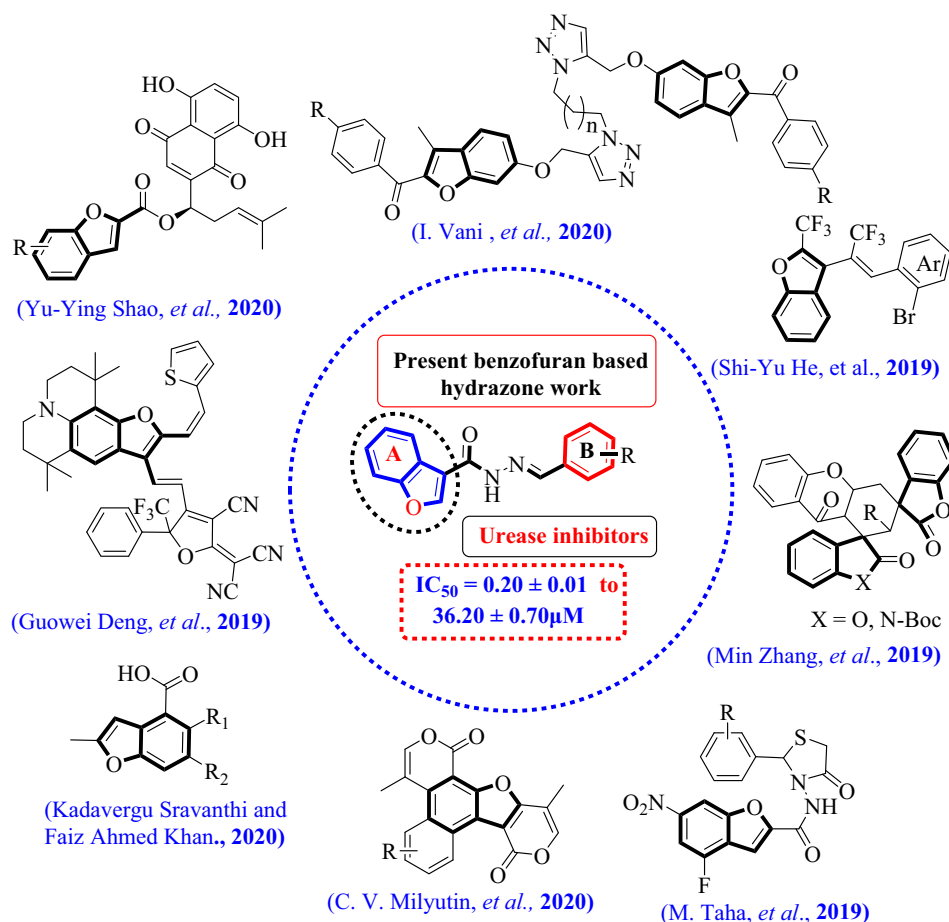


Fig. 2 Rational of the current study. (Deng et al., 2019; Milyutin et al., 2020; Sravanthi & Khan, 2020; Taha et al., 2020).

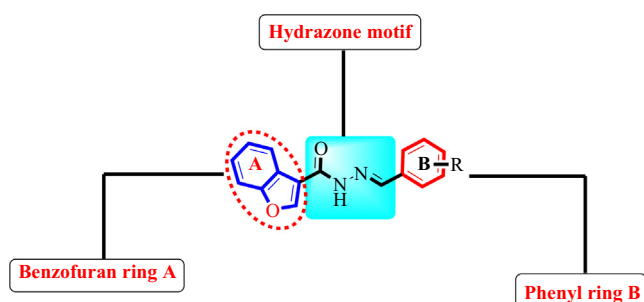


Fig. 3 General structure of benzoxazole bearing hydrazone scaffolds (1–25).

to remaining six carbons of benzofuran were observed at δ_{C-13} 159.5 (CH), 125.2 (C), 124.1 (CH), 122.5 (CH), 120.3 (CH) and 110.9 (CH) respectively. The peaks at δ_{C-13} 146.2 was observed for carbon involved in double bond with nitrogen atom (C = N).

3. Biological activity

3.1. *In vitro* urease inhibitory activity

All the newly synthesized benzofuran based hydrazone scaffolds (1–25) were subjected *in vitro* for their urease inhibitory

profile. It is noteworthy, that all the newly developed scaffolds illustrated moderate and good inhibition profile on evaluation against urease with IC_{50} values in the range of 0.20 ± 0.01 to $36.20 \pm 0.70 \mu M$ as compared to standard thiourea as reference inhibitor ($IC_{50} = 21.86 \pm 0.40 \mu M$). The general structural features of synthesized scaffolds are composed of benzofuran ring **A**, hydrazone moiety and substituted phenyl ring **B**. These parts play an important role in inhibition of urease enzymes. Variation in position, numbers, and nature of substituents around substituted phenyl ring **B** may be resultant to slight variation in inhibitory potentials of synthesized scaffolds.

3.1.1. Structure-activity relationship of urease inhibitory activity

All the synthetic scaffolds (1–25) were illustrated *in vitro* for their urease activity. Based on variation in the substitution pattern at phenyl ring **B**, limited structure-activity relationship was established. Analog **15** ($IC_{50} = 36.20 \pm 0.70 \mu M$) bearing *ortho*-methyl substitution on phenyl ring **B** was identified to exhibits the least inhibitory profile against urease enzymes among the synthesized scaffolds. Nonetheless, the analogues being substituted with hydroxyl group and fluoro groups illustrated good to excellent inhibitory profile than analog **15** showing that substitutions at phenyl ring **B** with hydroxyl groups and fluoro group enhance the inhibitory profile of the synthesized scaffolds. Nitro groups bearing ana-

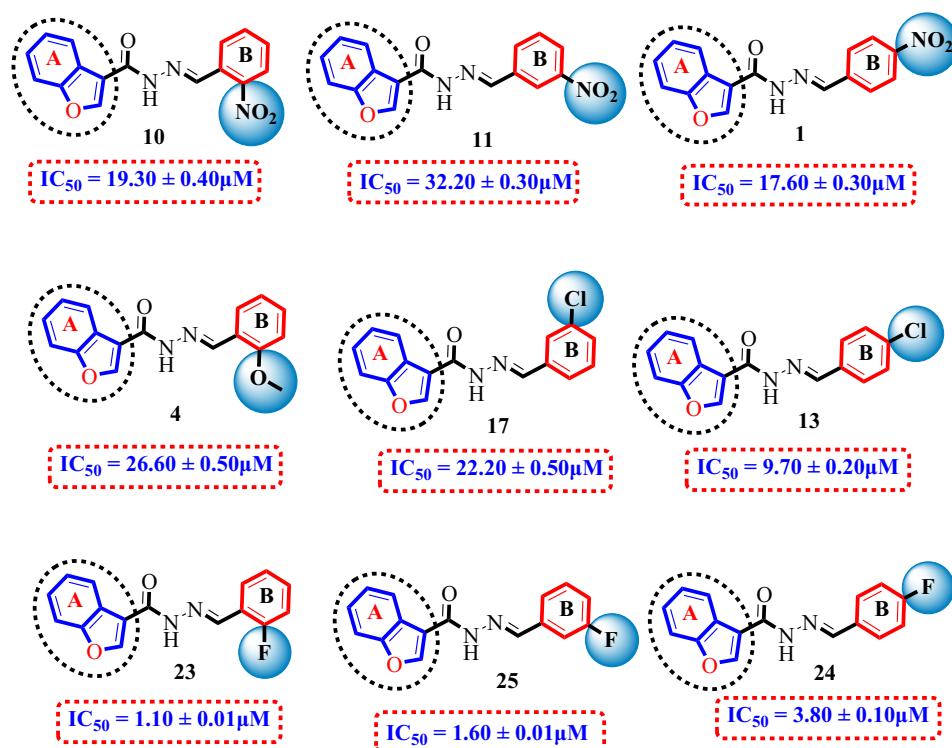


Fig. 4 SAR study of Halogen substituted analogues 1, 4, 10, 11, 13, 23-25 and 17.

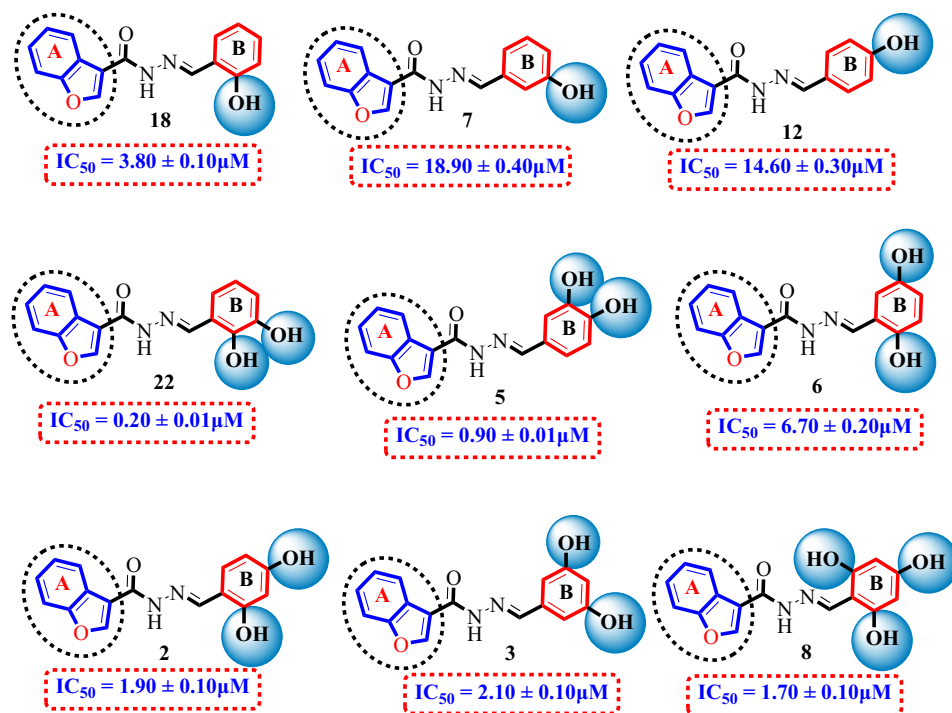
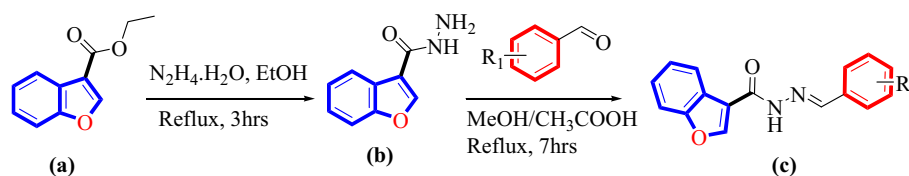


Fig. 5 SAR study of Analogue 2, 3, 5-8, 12, 18 and 22.

logues were found to display moderate to good inhibitory potentials. Among nitro substituted analogues, analogue **1** ($IC_{50} = 17.60 \pm 0.30 \mu M$) bearing *para*-nitro substitution at phenyl ring **B** was proved to be more active than its counterpart **10** ($IC_{50} = 19.30 \pm 0.40 \mu M$) bearing *ortho*-nitro substitution and **11** ($IC_{50} = 32.20 \pm 0.340 \mu M$) bearing *meta*-

nitro substitution at phenyl ring **B** against urease. This decline in *urease* activity of **10** ($IC_{50} = 19.30 \pm 0.40 \mu M$) bearing *ortho*-nitro substitution and **11** ($IC_{50} = 32.20 \pm 0.340 \mu M$) bearing *meta*-nitro substitution at phenyl ring **B** in comparison to analogue **1** may be due to shifting of nitro group from *para*-position of analogue **1** to either *ortho*-



Scheme 1 Synthesis of benzofuran based hydrazone derivatives.

position as in analogue **10** or *meta*-position as in analogue **11** at phenyl ring **B**.

Among halogen substituted analogues, analogues (**23–25**) bearing fluoro groups at different position of phenyl ring **B** displayed many folds more inhibitory profile in comparison to analogues (**13 and 17**) bearing chloro substitution at phenyl ring **B**. Among fluoro-substituted analogues, analogue **23** ($IC_{50} = 1.10 \pm 0.01 \mu\text{M}$) with *ortho*- fluoro substitution was seemed to be potent inhibitor of urease than its counterpart **24** ($IC_{50} = 3.80 \pm 0.10 \mu\text{M}$) and **25** ($IC_{50} = 1.60 \pm 0.01 \mu\text{M}$) bearing *para*- fluoro and *meta*-fluoro substitution at phenyl ring **B**. Analogue **23** ($IC_{50} = 1.10 \pm 0.01 \mu\text{M}$) bearing *ortho*-fluoro substitution at phenyl ring **B** against urease was identified to be the second most active analogues among the synthesized scaffolds. However, the analogues **24** and **25** bearing *para*-fluoro and *meta*-fluoro substitutions showed inferior inhibitory potentials as compared to analogue **23**. This decline in urease activity of analogue **24** ($IC_{50} = 3.80 \pm 0.10 \mu\text{M}$) and **25** ($IC_{50} = 1.60 \pm 0.01 \mu\text{M}$) bearing *para*-fluoro and *meta*-fluoro substitution at phenyl ring **B** in comparison to **23** ($IC_{50} = 1.10 \pm 0.01 \mu\text{M}$) with *ortho*-fluoro substitution may be due to shifting of fluoro group from its *ortho*-position to either *para*-position or *meta*-position as in analogues **24** and **25**. By comparing fluoro-substituted analogues **23** ($IC_{50} = 1.10 \pm 0.01 \mu\text{M}$), **24** ($IC_{50} = 3.80 \pm 0.10 \mu\text{M}$) and **25** ($IC_{50} = 1.60 \pm 0.01 \mu\text{M}$) with chloro-substituted analogues

13 ($IC_{50} = 9.70 \pm 0.20 \mu\text{M}$) and **17** ($IC_{50} = 22.20 \pm 0.50 \mu\text{M}$), the fluoro-substituted analogues displayed better urease inhibition in comparison to chloro-substituted analogues. Moreover, this discrepancy in activity of halogen-substituted analogues might be due to involvement of fluorine in hydrogen bonding with the active sites of enzyme as well as the electron-withdrawing effect offered by these substituents. Superior activity of fluoro-substituted analogues may be due to the stronger electron-withdrawing effect offered by fluorine in comparison to chloro- groups that offered weaker electron-withdrawing effect. So hence, the halogen-substituted analogues were showed urease activity in order of F-substitute $d > \text{Cl}$ -substituted analogues.

The addition of hydroxyl groups at various position of phenyl ring **B** such as *para*-position, *ortho*-position and *meta*-position of phenyl ring **B** as in analogue **12** ($IC_{50} = 14.60 \pm 0.30 \mu\text{M}$), **18** ($IC_{50} = 3.80 \pm 0.10 \mu\text{M}$) and **7** ($IC_{50} = 18.90 \pm 0.40 \mu\text{M}$) were identified to be favorable for urease inhibition, but analogue **18** ($IC_{50} = 3.80 \pm 0.10 \mu\text{M}$) were found to be many folds more active than standard thiourea as reference inhibitor ($IC_{50} = 21.86 \pm 0.40 \mu\text{M}$). However, the analogues **7** ($IC_{50} = 18.90 \pm 0.40 \mu\text{M}$) bearing *meta*-hydroxy substitution showed comparable urease activity as compared to reference inhibitor. A decline in urease activity was observed by shifting the hydroxyl group from *ortho*-position of analogue **18** to either *para*-position or *meta*-position as in analogues **12** and

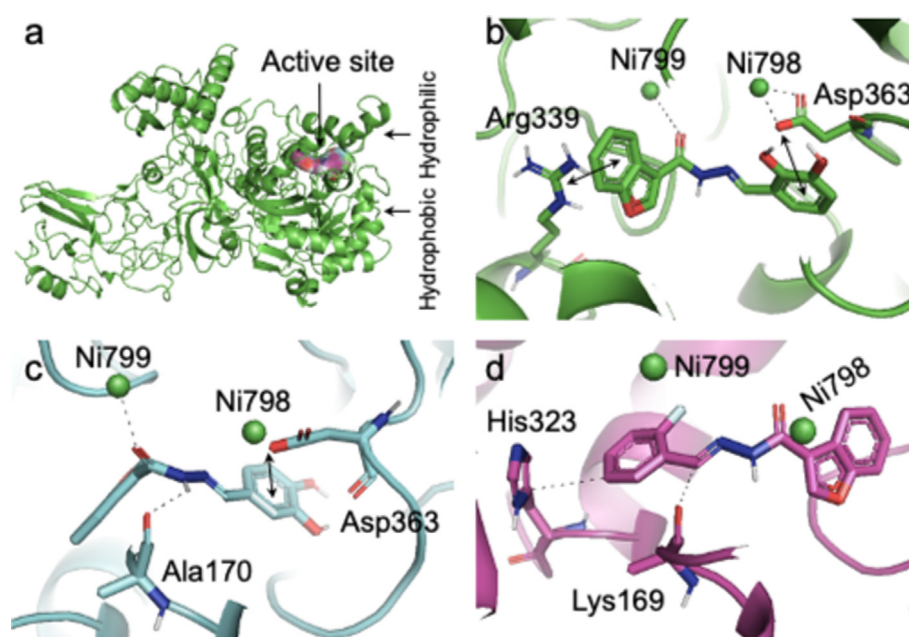


Fig. 6 The PLI profiles for active compounds in the series. (a) the cartonic representation of urease enzyme, (b) the mode of interaction for highly potent compound **22**, (c) for rank 2nd active compound **05**, and (d) for rank 3rd active compound **23**. Hydrogen bonding is shown in black color dotted lines, and the both sided arrows indicate the pi-stacking interaction.

Table 2 The PLI profile for potent compounds.

Compound	Ligand	Receptor	Interaction	Distance	E (kcal/mol)	Docking score			
22	NI	798	OQ1	KCX	220	Metal	2.06	-8.0	-7.2759881
	NI	798	NE2	HIS	275	Metal	2.23	-1.4	
	NI	798	O	GLY	280	Metal	2.20	-3.1	
	NI	798	O	GLY	281	Metal	2.25	-3.2	
	NI	799	NE2	HIS	139	Metal	2.25	-3.3	
	NI	799	OQ2	KCX	220	Metal	2.07	-6.9	
	NI	799	OD1	ASP	363	Metal	2.07	-5.4	
	NI	799	OD2	ASP	363	Metal	2.15	-5.0	
	NI	798	OQ1	KCX	220	Ionic	2.06	-15.1	
	NI	799	OQ2	KCX	220	Ionic	2.07	-14.9	
	NI	799	OD1	ASP	363	Ionic	2.07	-14.9	
	NI	799	OD2	ASP	363	Ionic	2.15	-13.6	
	5-ring		NH2	ARG	339	pi-cation	3.54	-3.8	
6-ring		CB	ASP	363	pi-H	3.79	-0.7		
05	N	12	O	ALA	170	H-donor	3.05	-0.5	-6.96462822
	O	11	NI	NI	798	Metal	2.62	-1.0	
	NI	798	OQ1	KCX	220	Metal	2.06	-8.0	
	NI	798	NE2	HIS	275	Metal	2.23	-1.4	
	NI	798	O	GLY	280	Metal	2.20	-3.1	
	NI	798	O	GLY	281	Metal	2.25	-3.2	
	NI	799	NE2	HIS	139	Metal	2.25	-3.3	
	NI	799	OQ2	KCX	220	Metal	2.07	-6.9	
	NI	799	OD1	ASP	363	Metal	2.07	-5.4	
	NI	799	OD2	ASP	363	Metal	2.15	-5.0	
6-ring		CB	ASP	363	pi-H	4.00	-0.5		
23	N	12	O	LYS	169	H-donor	3.70	-0.5	-6.4081377
	NI	799	OD2	ASP	363	Ionic	2.15	-13.6	
	C	17	5-ring	HIS	323	H-pi	3.67	-0.5	

7. It was concluded that substitution of hydroxyl group at *ortho*-position of phenyl ring may influence the activity.

It was suggested by the SAR study that alteration in numbers of hydroxyl groups around phenyl ring **B** has proven to be encouraging for the inhibition of urease enzyme. By comparing analogues **22** ($IC_{50} = 0.20 \pm 0.001 \mu M$), bearing two hydroxyl groups at *ortho*- and *meta*-position respectively, with analogue **7** ($IC_{50} = 5.20 \pm 0.10 \mu M$) and **12** ($IC_{50} = 14.60 \pm 0.30 \mu M$) bearing only one hydroxyl group at *meta*-position and *para*-position of phenyl ring **B**, analogue **22** ($IC_{50} = 0.20 \pm 0.001 \mu M$) showed many folds better inhibitory profile. This elevated urease activity of analogue **22** ($IC_{50} = 0.20 \pm 0.001 \mu M$), in comparison to analogue **7** ($IC_{50} = 5.20 \pm 0.10 \mu M$) and **12** ($IC_{50} = 14.60 \pm 0.30 \mu M$) might be due the presence of two hydroxyl groups that may interact better through hydrogen bonding with active site of enzyme.

3.2. Docking study

3.2.1. Results and discussion

In order to explore the binding pattern of all synthesized compounds within the active site of the urease enzyme, a molecular docking study was conducted using the default parameters implemented in the MOE modeling software. As illustrated in Fig. 6a, the active site of the urease enzyme contains both hydrophilic and hydrophobic regions. In addition, the crystal

structure of the urease enzyme contained one KCX-220 modified tyrosine residue and two nickel ions in their active cavity, which compete for a prominent role by binding essential amino acids with ligands and triggering urease activity. However, the docking analysis revealed that all of the compounds had a similar pattern of binding in the active region of the urease enzyme. Following that, based on docking score and interaction profile, the most promising docked conformation of each compound was further examined for PLI profile analysis. It has been observed that all the compounds carrying various substituted groups at benzene ring (i.e., electron withdrawing (EWG), and donating (EDG) groups), hence, this variation in groups, their quantity, and its position eventually impact the urease activity.

In the case of the most active derivative **22** in the series, which carried EDG, the PLI profile revealed mostly favorable ionic and other interactions (i.e. hydrogen bond, etc.) with the catalytic residues, as shown in Fig. 1b, not only with the key residues, but also with the Ni ion, which played a key role in enhancing the enzyme's activity. The great potency of this molecule could be attributable to the attached EDG (also known as an activating group), their quantity at the benzene ring, which further fully stabilized the ring and donated much of its electronic density to the reaction centre, or also the strong magnitude activation (hydroxy group). Another reason for the high potency could be the ionic interaction with the Ni

ion, which helps to boost activity. Other compounds with single EDG at various positions, such as compound 23, 05, and others, also showed sufficient strength against the urease enzyme. The lower potency compared to compound 22 could be attributed to reduced electronic density donation to the reaction centre, and one major reason could be the series' weak magnitude of donating groups. Fig. 6c and Fig. 6d demonstrate the PLI profile of these compounds. Furthermore, the experimental results based on numerous interactions of compounds with critical residues of the urease enzyme are strongly supported by the molecular docking studies. The current molecular docking data show that the quantity of substituted groups, their position, and the magnitude of their activation and deactivation all have a significant impact on enzyme activity. The protein–ligand interaction (PLI) profile for potent compounds has been listed in Table 2. The ionic and metal interaction included in the table just for the ease of comparison of the ranked 1st, 2nd and 3rd compound in the series. These were the stabilized interactions which provided additional stability to the reaction center where needed.

4. Conclusion

In conclusion, we have established a facile protocol for the synthesis of benzofuran based hydrazone via dehydrative condensation of benzofuran based hydrazide and corresponding benzaldehyde in methanol along with few drops of glacial acetic acid. The scope and diversity of this practical synthetic approach works well with variety of benzaldehyde substrates. The features such as simple operation, high efficiency, mild reaction condition and short reaction time make it valuable alternative for the synthesis of benzofuran based hydrazone. Spectroscopic techniques such as ^1H NMR, ^{13}C NMR and HR-MS were used to characterize the newly afforded analogues. Furthermore, according to literature known protocol, hybrid scaffolds (**1–25**) of benzofuran based hydrazone were evaluated *in vitro*, for their urease inhibition. All the newly afforded compounds were found to show moderate to good inhibitory activity against urease enzyme, when compared to standard thiourea. Compounds bearing either hydroxy or fluoro groups on ph-ring were identified as the most active competitor of urease enzyme owing to involvement of these substituent in H-bonding with active site of urease enzyme. In addition, the molecular docking study was also conducted to explore the interactions of synthetic compounds with urease active site and results supported the experimental data.

5. Material and methods

5.1. General procedure of benzofuran based hydrazone analogues (1–25)

The ethyl benzofuran-3-carboxylate (**a**) (5 g, 26.3 mmol) was taken in ethanol and hydrazine hydrate mixture 50 (1:1). The reaction mixture refluxed for about 3hrs to get the benzofuran-3-carbohydrazide as a starting material (**b**). In the next step, the benzofuran-3-carbohydrazide (1 mmol,

0.176 g) (**b**) was treated with various corresponding benzaldehyde (1mmole) in methanol (10 mL) along with few drops of glacial acetic acid and the reaction mixture put under reflux until the reaction completed the progress of the reaction was monitored by TLC. The solvent was evaporated and resulting solid residue washing with n-hexane and recrystallized in methanol to afford the synthesis of desired benzofuran based hydrazone scaffolds (**1–25**) in excellent yield.

5.2. (*E*)-*N'*-(4-nitrobenzylidene) benzofuran-3-carbohydrazide (1)

^1H NMR (500 MHz, DMSO d_6): δ 12.36 (s, 1H, –NH), 8.65 (s, 1H, H-2), 8.32 (d, J ($2'$, $3'/6'$, $5'$) = 6.9 Hz, 2H, H-2'/H-6'), 7.98 (d, J ($3'$, $2'/5'$, $6'$) = 7.7 Hz, 2H, H-3'/H-5'), 7.82 (dd, J ($4/5$) = 7.4 Hz, J ($4/6$) = 1.9 Hz, 1H, H-4), 7.67–7.64 (m, 1H, H-5), 7.56 (dt, J ($6/5,7$) = 9.0 Hz, J ($6/4$) = 2.0 Hz, 1H, H-6), 7.39 (d, J ($7/6$) = 2.2 Hz, 1H, H-7), 7.38 (s, 1H, –HC-N); ^{13}C NMR (125 MHz, DMSO d_6): δ 162.2, 159.1, 155.3, 150.6, 145.8, 140.1, 124.8, 124.5, 124.5, 124.3, 124.3, 123.7, 122.3, 122.1, 119.9, 110.5, HREI-MS: m/z [M + H] $^+$ calcd for $\text{C}_{16}\text{H}_{11}\text{N}_3\text{O}_4$ 309.0745, found 309.0740.

5.3. (*E*)-*N'*-(2,4-dihydroxybenzylidene) benzofuran-3-carbohydrazide (2)

^1H NMR (500 MHz, DMSO d_6): δ 12.02 (s, 1H, –NH), 11.5 (br, s, 1H, –OH), 10.0 (br, s, 1H, –OH), 8.60 (s, 1H, H-2), 7.80 (s, 1H, –HC-N), 7.79 (dd, J ($4/5$) = 7.0 Hz, 1H, H-4), 7.54 (d, J ($6'$, $5'$) = 6.3 Hz, 1H, H-6'), 7.51 (d, J ($7/6$) = 7.2 Hz, 1H, H-7), 7.42 (d, J ($3'$, $5'$) = 2.4 Hz, 1H, H-3'), 7.39 (dt, J ($6/5,7$) = 9.1 Hz, J ($6/4$) = 2.1 Hz, 1H, H-6), 7.37–7.27 (m, 1H, H-5), 6.40 (d, J ($5'$, $6'$) = 7.5 Hz, 1H, H-5'); ^{13}C NMR (125 MHz, DMSO d_6): δ 162.8, 162.6, 162.4, 159.3, 155.5, 146.0, 134.1, 125.0, 123.9, 122.5, 122.3, 120.1, 111.4, 110.7, 108.9, 104.0; HREI-MS: m/z [M + H] $^+$ calcd for $\text{C}_{16}\text{H}_{12}\text{N}_2\text{O}_4$ 296.0793, found 296.0787.

5.4. (*E*)-*N'*-(3,5-dihydroxybenzylidene) benzofuran-3-carbohydrazide (3)

^1H NMR (500 MHz, DMSO d_6): δ 12.36 (s, 1H, –NH), 10.71 (s, 1H, –OH), 10.03 (s, 1H, –OH), 8.72 (s, 1H, H-2), 8.32 (s, 1H, –HC-N), 7.81 (d, J ($4/5$) = 7.6 Hz, 1H, H-4), 7.54 (d, J ($7/6$) = 6.5 Hz, 1H, H-7), 7.55 (t, J ($6/5$) = 9.2 Hz, J ($6/4$) = 2.3 Hz, 1H, H-6), 7.66 (d, J ($5/4$) = 7.6 Hz, 1H, H-5), 7.40 (t, J ($6'/2'$, $4'$) = 1.8 Hz, 1H, H-6'), 7.09 (d, J ($2'$, $4'$) = 2.0 Hz, 1H, H-2'), 6.93 (dd, J ($4'$, $2'$) = 2.4 Hz, J ($4'$, $6'$) = 2.8 Hz, 1H, H-4'); ^{13}C NMR (125 MHz, DMSO d_6): δ 162.6, 160.3, 160.3, 159.5, 155.7, 146.2, 136.8, 125.2, 124.1, 122.7, 122.5, 120.3, 110.9, 107.8, 107.8, 106.2; HREI-MS: m/z [M + H] $^+$ calcd for $\text{C}_{16}\text{H}_{12}\text{N}_2\text{O}_4$ 296.0793, found 296.0787.

5.5. (*E*)-*N'*-(2-methoxybenzylidene) benzofuran-3-carbohydrazide (4)

^1H NMR (500 MHz, DMSO d_6): δ 12.28 (s, 1H, –NH), 11.64 (s, 1H, H-2), 8.65 (s, 1H, –HC-N), 7.81 (d, J ($7/6$) = 8.2 Hz, 1H,

H-7), 7.66 (d, $J_{(4/5)} = 7.4$ Hz, 1H, H-4), 7.55–7.52 (m, 1H, H-2'), 7.40–7.37 (m, 3H, H-3'/H-4'/H-5'), 6.55–6.51 (m, 2H, H-5/H-6), 3.78 (s, 3H, –OCH₃); ¹³C NMR (125 MHz, DMSO d_6): δ 162.3, 159.2, 157.9, 155.4, 145.9, 132.3, 132.0, 124.9, 123.8, 122.4, 122.2, 121.4, 120.0, 117.2, 111.5, 110.6; HREI-MS: m/z [M + H]⁺ calcd for C₁₇H₁₄N₂O₃ 294.1000, found 294.0991.

5.6. (*E*)-*N'*-(3,4-dihydroxybenzylidene)benzofuran-3-carbohydrazide (5)

¹H NMR (500 MHz, DMSO d_6): δ 12.23 (s, 1H, –NH), 11.51 (br, s, 1H, –OH), 9.51 (br, s, 1H, –OH), 8.57 (s, 1H, H-2), 8.45 (s, 1H, –HC-N), 7.80 (d, $J_{(4/5)} = 8.4$ Hz, 1H, H-4), 7.66 (d, $J_{(7/6)} = 6.5$ Hz, 1H, H-7), 7.54–7.52 (m, 1H, H-5), 7.40 (t, $J_{(6/5,7)} = 7.9$ Hz, 1H, H-6), 7.29 (d, $J_{(2', 6')} = 1.8$ Hz, 1H, H-2'), 6.76 (d, $J_{(5', 6')} = 7.3$ Hz, 1H, H-3'), 6.41 (d, $J_{(6', 2')} = 2.6$ Hz, 1H, H-6'); ¹³C NMR (125 MHz, DMSO d_6): δ 162.5, 159.4, 155.6, 149.9, 146.4, 146.1, 131.6, 125.1, 124.0, 123.5, 122.6, 122.4, 120.2, 117.7, 116.6, 110.8, HREI-MS: m/z [M + H]⁺ calcd for C₁₆H₁₂N₂O₄ 296.0793, found 296.0787.

5.7. (*E*)-*N'*-(2,5-dihydroxybenzylidene)benzofuran-3-carbohydrazide (6)

¹H NMR (500 MHz, DMSO d_6): δ 12.25 (s, 1H, –NH), 10.41 (s, 2H, –OH), 9.0 (s, 1H, H-2), 8.67 (s, 1H, –HC-N), 7.81 (dd, $J_{(4/5)} = 6.4$ Hz, 1H, H-4), 7.66 (d, $J_{(7/6)} = 7.8$ Hz, 1H, H-7), 7.40 (t, $J_{(6/5,7)} = 6.9$ Hz, 1H, H-6), 7.55–7.52 (m, 1H, H-5), 6.94 (d, $J_{(2', 4')} = 2.7$ Hz, 1H, H-2'), 6.77–6.74 (dd, $J_{(4', 5')} = 6.9$ Hz, $J_{(4', 2')} = 1.9$ Hz, 1H, H-4'), 6.73 (d, $J_{(5', 4')} = 7.9$ Hz, 1H, H-5'); ¹³C NMR (125 MHz, DMSO d_6): δ 162.7, 159.6, 155.8, 154.0, 151.5, 146.3, 125.3, 124.2, 122.8, 122.6, 120.7, 120.4, 120.2, 119.9, 116.6, 111.0; HREI-MS: m/z [M + H]⁺ calcd for C₁₆H₁₂N₂O₄ 296.0793, found 296.0787.

5.8. (*E*)-*N'*-(3-hydroxybenzylidene) benzofuran-3-carbohydrazide (7)

¹H NMR (500 MHz, DMSO d_6): δ 12.06 (s, 1H, –NH), 9.67 (s, 1H, –OH), 8.47 (s, 1H, H-2), 8.43 (s, 1H, –HC-N), 7.80 (d, $J_{(4/5)} = 7.4$ Hz, 1H, H-4), 7.66 (d, $J_{(7/6)} = 7.6$ Hz, 1H, H-7), 7.54 (t, $J_{(2'/4', 6')} = 2.6$ Hz, 1H, H-2'), 7.39 (t, $J_{(5'/4', 6')} = 7.8$ Hz, 1H, H-5'), 7.28 (d, $J_{(6', 5')} = 6.6$ Hz, 1H, H-6'), 7.25–7.09 (m, 2H, H-5/H-6), 6.85 (d, $J_{(4', 5')} = 6.8$ Hz, 1H, H-4'); ¹³C NMR (125 MHz, DMSO d_6): δ 162.9, 159.8, 158.9, 156.0, 146.5, 139.0, 130.5, 125.5, 124.4, 123.0, 122.8, 122.1, 120.6, 118.5, 115.2, 111.2, HREI-MS: m/z [M + H]⁺ calcd for C₁₆H₁₂N₂O₃ 280.0842, found 280.0835.

5.9. (*E*)-*N'*-(2,4,6-trihydroxybenzylidene)benzofuran-3-carbohydrazide (8)

¹H NMR (500 MHz, DMSO d_6): δ 12.19 (s, 1H, –NH), 11.11 (br, s, 2H, –OH), 9.85 (br, s, 1H, –OH), 8.90 (s, 1H, H-2), 8.57 (s, 1H, –HC-N), 7.79 (d, $J_{(4/5)} = 1.2$ Hz, 1H, H-3'), 7.78 (d, $J_{(5/4,6)} = 1.9$ Hz, 1H, H-5'), 7.51 (t, $J_{5(4,6) / 6(5,7)} = 8.2$ Hz, 2H, H-5/H-6), 7.33 (dd, $J_{(4, 5)/(7,6)} = 8.0$ Hz, $J_{(4, 6)/(7,4)} = 2.4$ Hz, 2H, H-4/H-7); ¹³C NMR (125 MHz,

DMSO d_6): δ 164.2, 164.2, 163.9, 163.0, 159.9, 156.1, 146.6, 125.6, 124.5, 123.1, 122.9, 120.7, 111.3, 106.5, 101.1, 101.1; HREI-MS: m/z [M + H]⁺ calcd for C₁₆H₁₂N₂O₅ 312.0741, found 312.0733.

5.10. (*E*)-*N'*-(4-(dimethylamino) benzylidene) benzofuran-3-carbohydrazide (9)

¹H NMR (500 MHz, DMSO d_6): δ 11.91 (s, 1H, –NH), 8.50 (s, 1H, H-2), 8.36 (s, 1H, –HC-N), 7.79 (d, $J_{(2', 3'/ 6', 5')} = 7.8$ Hz, 2H, H-2'/H-6'), 7.68 (dd, $J_{(4, 5)/(7,6)} = 8.0$ Hz, $J_{(4, 6)/(7,4)} = 2.4$ Hz, 2H, H-4/H-7), 7.54 (t, $J_{5(4,6)} = 8.2$ Hz, 1H, H-5), 7.39 (t, $J_{6(5,7)} = 8.2$ Hz, 1H, H-6), 7.05 (d, $J_{(3', 2'/5', 6')} = 8.1$ Hz, 2H, H-3'/H-5'), 3.37 (s, 6H, –CH₃); ¹³C NMR (125 MHz, DMSO d_6): δ 163.1, 160.0, 156.2, 153.7, 146.7, 128.6, 128.6, 125.7, 124.6, 123.5, 123.2, 123.0, 120.8, 112.2, 112.2, 111.4, 41.6, 41.6; HREI-MS: m/z [M + H]⁺ calcd for C₁₈H₁₇N₃O₂ 307.1318, found 307.1311.

5.11. (*E*)-*N'*-(2-nitrobenzylidene) benzofuran-3-carbohydrazide (10)

¹H NMR (500 MHz, DMSO d_6): δ 12.36 (s, 1H, –NH), 9.09 (s, 1H, H-2), 8.04 (s, 1H, –HC-N), 7.55–7.53 (m, 3H, H-3'/H-5'/H-6'), 7.81 (dd, $J_{(4/5)} = 7.4$ Hz, $J_{(4/6)} = 2.4$ Hz, 1H, H-4), 7.40 (t, $J_{(4'/5', 3')} = 9.0$ Hz, 1H, H-4'), 7.47–7.45 (m, 3H, H-5/H-6/H-7); ¹³C NMR (125 MHz, DMSO d_6): δ 162.8, 159.7, 155.9, 148.1, 146.4, 135.2, 132.2, 130.4, 128.7, 125.4, 124.3, 124.1, 122.9, 122.7, 120.5, 111.1, HREI-MS: m/z [M + H]⁺ calcd for C₁₆H₁₁N₃O₄ 309.0745, found 309.0740.

5.12. (*E*)-*N'*-(3-nitrobenzylidene) benzofuran-3-carbohydrazide (11)

¹H NMR (500 MHz, DMSO d_6): δ 12.31 (s, 1H, –NH), 8.67 (s, 1H, H-2), 8.54 (s, 1H, –HC-N), 8.29 (d, $J_{(2', 4')} = 2.6$ Hz, 1H, H-2'), 8.27 (dd, $J_{(6', 5')} = 6.8$ Hz, $J_{(6', 4')} = 1.6$ Hz, 1H, H-6'), 7.80–7.76 (m, 2H, H-4'/H-5'), 7.81 (dd, $J_{(4/5)} = 7.4$ Hz, 1H, H-4), 7.67 (d, $J_{(7/6)} = 7.4$ Hz, 1H, H-7), 7.41–7.38 (m, 2H, H-5/H-6); ¹³C NMR (125 MHz, DMSO d_6): δ 162.2, 159.1, 155.3, 148.3, 145.8, 134.9, 132.8, 130.0, 126.6, 124.8, 123.7, 122.3, 122.1, 121.9, 119.9, 110.5, HREI-MS: m/z [M + H]⁺ calcd for C₁₆H₁₁N₃O₄ 309.0745, found 309.0740.

5.13. (*E*)-*N'*-(4-hydroxybenzylidene) benzofuran-3-carbohydrazide (12)

¹H NMR (500 MHz, DMSO d_6): δ 11.84 (s, 1H, –NH), 9.96 (s, 1H, –OH), 8.44 (s, 1H, H-2), 8.29 (s, 1H, –HC-N), 7.79 (dd, $J_{(4/5)} = 7.0$ Hz, 1H, H-4), 7.64 (d, $J_{(2', 3'/ 6', 5')} = 7.0$ Hz, 2H, H-2'/H-6'), 7.56–7.50 (m, 2H, H-6/H-7), 7.39 (t, $J_{(5/4,6)} = 6.6$ Hz, 1H, H-5), 6.85 (d, $J_{(3', 2'/5', 6')} = 8.2$ Hz, 2H, H-3'/H-5'); ¹³C NMR (125 MHz, DMSO d_6): δ 162.4, 161.1, 159.3, 155.5, 146.0, 130.9, 130.9, 126.6, 125.0, 123.9, 122.5, 122.3, 120.1, 116.3, 116.3, 110.7; HREI-MS: m/z [M + H]⁺ calcd for C₁₆H₁₂N₂O₃ 280.0842, found 280.0835.

5.14. (*E*)-*N'*-(4-chlorobenzylidene) benzofuran-3-carbohydrazide (13)

¹H NMR (500 MHz, DMSO *d*₆): δ 12.15 (s, 1H, –NH), 8.55 (s, 1H, H-2), 8.32 (s, 1H, –HC-N), 7.55–7.52 (m, 4H, H-2'/H-3'/H-5'/H-6'), 7.75 (d, *J*_(4, 5/5,4) = 7.6 Hz, 2H, H-4/H-5), 7.80 (d, *J*_(7/6) = 7.5 Hz, 1H, H-7), 7.40 (t, *J*_(6/5,7) = 9.2 Hz, 1H, H-6); ¹³C NMR (125 MHz, DMSO *d*₆): δ 162.6, 159.5, 155.7, 146.2, 136.9, 132.1, 130.9, 130.9, 129.2, 129.2, 125.2, 124.1, 122.7, 122.5, 120.3, 110.9; HREI-MS: *m/z* [M + H]⁺ calcd for C₁₆H₁₁N₂O₂Cl 298.0503, found 298.0494.

5.15. Methyl (*E*)-4-((2-(benzofuran-3-carbonyl) hydrazono) methyl) benzoate (14)

¹H NMR (500 MHz, DMSO *d*₆): δ 11.31 (s, 1H, –NH), 8.58 (s, 1H, H-2), 8.28 (s, 1H, –HC-N), 7.75 (d, *J*_(4/5) = 7.4 Hz, 1H, H-4), 7.05 (d, *J*_(7/6) = 7.7 Hz, 1H, H-7), 7.68–7.64 (m, 4H, H-2'/H-3'/H-5'/H-6'), 7.54 (t, *J*_(6/5,7) = 9.0 Hz, 1H, H-6), 7.39 (t, *J*_(5/6,7) = 9.0 Hz, 1H, H-5), 3.8 (s, 3H, –OCH₃); ¹³C NMR (125 MHz, DMSO *d*₆): δ 166.2, 162.3, 159.2, 155.4, 145.9, 138.3, 132.7, 130.3, 130.3, 129.4, 129.4, 124.9, 123.8, 122.4, 122.2, 120.0, 110.6, 51.8; HREI-MS: *m/z* [M + H]⁺ calcd for C₁₈H₁₄N₂O₄ 322.0948, found 322.0939.

5.16. (*E*)-*N'*-(2-methylbenzylidene) benzofuran-3-carbohydrazide (15)

¹H NMR (500 MHz, DMSO *d*₆): δ 12.05 (s, 1H, –NH), 8.89 (s, 1H, H-2), 8.33 (s, 1H, –HC-N), 7.86 (d, *J*_(6', 5') = 7.0 Hz, 1H, H-6'), 7.80 (d, *J*_(7/6) = 7.5 Hz, 1H, H-7), 7.66 (d, *J*_(4/5) = 8.4 Hz, 1H, H-4), 7.54 (t, *J*_(5/4,6) = 7.9 Hz, 1H, H-5), 7.40 (t, *J*_(6/5,7) = 7.6 Hz, 1H, H-6), 7.34–7.26 (m, 3H, H-3'/H-4'/H-5'), 2.46 (s, 3H, –CH₃); ¹³C NMR (125 MHz, DMSO *d*₆): δ 162.5, 159.4, 155.6, 146.1, 135.8, 131.4, 131.2, 129.3, 126.8, 126.0, 125.1, 124.0, 122.6, 122.4, 120.2, 110.8, 19.3; HREI-MS: *m/z* [M + H]⁺ calcd for C₁₇H₁₄N₂O₂ 278.1050, found 278.1044.

5.17. (*E*)-*N'*-(4-methylbenzylidene) benzofuran-3-carbohydrazide (16)

¹H NMR (500 MHz, DMSO *d*₆): δ 12.00 (s, 1H, –NH), 8.53 (s, 1H, H-2), 8.30 (s, 1H, –HC-N), 7.79 (d, *J*_(4/5) = 6.4 Hz, 1H, H-4), 7.66 (d, *J*_(7/6) = 7.2 Hz, 1H, H-7), 7.63 (d, *J*_(2', 3'/6', 5') = 7.8 Hz, 2H, H-2'/H-6'), 7.54 (t, *J*_(5/4,6) = 7.9 Hz, 1H, H-5), 7.39 (t, *J*_(6/5,7) = 7.6 Hz, 1H, H-6), 7.29 (d, *J*_(3', 2'/5', 6') = 8.1 Hz, 2H, H-3'/H-5'), 2.35 (s, 3H, –CH₃); ¹³C NMR (125 MHz, DMSO *d*₆): δ 162.7, 159.6, 155.8, 146.3, 141.0, 131.0, 129.4, 129.4, 126.4, 126.4, 125.3, 124.2, 122.8, 122.6, 120.4, 111.0, 22.5; HREI-MS: *m/z* [M + H]⁺ calcd for C₁₇H₁₄N₂O₂ 278.1050, found 278.1044.

5.18. (*E*)-*N'*-(3-chlorobenzylidene) benzofuran-3-carbohydrazide (17)

¹H NMR (500 MHz, DMSO *d*₆): δ 12.21 (s, 1H, –NH), 8.54 (s, 1H, H-2), 8.34 (s, 1H, –HC-N), 7.68 (t, *J*_(2'/4', 6') = 2.6 Hz, 1H,

H-2'), 7.66 (d, *J*_(6', 5') = 6.8 Hz, 1H, H-6'), 7.40–7.37 (m, 1H, H-4'), 7.81 (t, *J*_(5'/4', 6') = 7.8 Hz, 1H, H-5'), 7.55–5.0 (m, 4H, H-4/H-5/H-6/H-7); ¹³C NMR (125 MHz, DMSO *d*₆): δ 162.9, 159.8, 156.0, 146.5, 135.4, 134.7, 131.4, 130.5, 127.6, 127.4, 125.5, 124.4, 123.0, 122.8, 120.6, 111.2; HREI-MS: *m/z* [M + H]⁺ calcd for C₁₆H₁₁N₂O₂Cl 298.0503, found 298.0494.

5.19. (*E*)-*N'*-(2-hydroxybenzylidene) benzofuran-3-carbohydrazide (18)

¹H NMR (500 MHz, DMSO *d*₆): δ 12.34 (s, 1H, –NH), 11.37 (s, 1H, –OH), 8.75 (s, 1H, H-2), 8.31 (s, 1H, –HC-N), 7.81 (d, *J*_(4/5) = 8.2 Hz, 1H, H-4), 7.67 (d, *J*_(7/6) = 7.8 Hz, 1H, H-7), 7.55–7.51 (m, 2H, H-5/H-6), 7.40 (d, *J*_(5', 4') = 7.2 Hz, 1H, H-5'), 7.38–7.30 (m, 1H, H-6'), 6.95 (t, *J*_{(3'(2', 4')/(4'(3', 5'))} = 9.0 Hz, 2H, H-3'/H-4'); ¹³C NMR (125 MHz, DMSO *d*₆): δ 163.0, 159.9, 157.5, 156.1, 146.6, 132.7, 127.8, 125.6, 124.5, 123.1, 122.9, 121.7, 120.7, 118.8, 118.2, 111.3; HREI-MS: *m/z* [M + H]⁺ calcd for C₁₆H₁₂N₂O₃ 280.0842, found 280.0835.

5.20. (*E*)-*N'*-(3-methylbenzylidene) benzofuran-3-carbohydrazide (19)

¹H NMR (500 MHz, DMSO *d*₆): δ 12.07 (s, 1H, –NH), 8.52 (s, 1H, H-2), 8.36 (s, 1H, –HC-N), 7.80 (d, *J*_(4/5) = 7.7 Hz, 1H, H-4), 7.66 (d, *J*_(7/6) = 7.4 Hz, 1H, H-7), 7.55–7.50 (m, 2H, H-5/H-6), 7.39–7.35 (m, 3H, H-4'/H-5'/H-6'), 7.27 (d, *J*_(2'/4') = 2.0 Hz, 1H, H-2'), 2.37 (s, 3H, –CH₃); ¹³C NMR (125 MHz, DMSO *d*₆): δ 163.1, 160.0, 156.2, 146.7, 138.8, 133.9, 131.6, 129.7, 129.0, 126.5, 125.7, 124.6, 123.2, 123.0, 120.8, 111.4, 21.8; HREI-MS: *m/z* [M + H]⁺ calcd for C₁₇H₁₄N₂O₂ 278.1050, found 278.1044.

5.21. (*E*)-*N'*-(3-hydroxy-4-methoxybenzylidene) benzofuran-3-carbohydrazide (20)

¹H NMR (500 MHz, DMSO *d*₆): δ 11.89 (s, 1H, –NH), 9.34 (s, 1H, –OH), 8.40 (s, 1H, H-2), 8.35 (s, 1H, –HC-N), 7.79 (d, *J*_(4/5) = 7.4 Hz, 1H, H-4), 7.65 (d, *J*_(7/6) = 7.2 Hz, 1H, H-7), 7.53 (dd, *J*_(6', 5') = 7.6 Hz, *J*_(6', 2') = 2.6 Hz, 1H, H-6'), 7.39–7.26 (m, 1H, H-5/H-6), 7.05–6.99 (m, 2H, H-2'/H-5'), 3.81 (s, 3H, –OCH₃); ¹³C NMR (125 MHz, DMSO *d*₆): δ 162.8, 159.7, 155.9, 152.7, 147.6, 146.4, 131.3, 125.4, 124.3, 123.2, 122.9, 122.7, 120.5, 116.2, 112.6, 111.1, 56.7; HREI-MS: *m/z* [M + H]⁺ calcd for C₁₇H₁₄N₂O₄ 310.0950, found 310.0943.

5.22. (*E*)-*N'*-(2,4-dimethoxybenzylidene) benzofuran-3-carbohydrazide (21)

¹H NMR (500 MHz, DMSO *d*₆): δ 11.99 (s, 1H, –NH), 8.48 (s, 1H, H-2), 8.30 (s, 1H, –HC-N), 7.79 (d, *J*_(4/5) = 6.4 Hz, 1H, H-4), 7.65 (d, *J*_(7/6) = 2.1 Hz, 1H, H-7), 7.53 (t, *J*_(5', 4'/6', 3') = 7.5 Hz, 1H, H-5'), 7.39–7.35 (m, 2H, H-5/H-6), 7.20 (d, *J*_(6', 5') = 6.3 Hz, 1H, H-6'), 7.05 (d, *J*_(3', 5') = 2.4 Hz, 1H, H-3'), 3.83 (s, 3H, –OCH₃), 3.81 (s, 3H, –OCH₃); ¹³C NMR

(125 MHz, DMSO d_6): δ 164.2, 162.7, 159.8, 159.6, 155.8, 146.3, 133.3, 125.3, 124.2, 122.8, 122.6, 120.4, 111.0, 109.5, 107.0, 101.8, 56.3, 56.1; HREI-MS: m/z [M + H]⁺ calcd for C₁₈H₁₆N₂O₄ 324.1105, found 324.1100.

5.23. (*E*)-*N'*-(2,3-dihydroxybenzylidene)benzofuran-3-carbohydrazide (22)

¹H NMR (500 MHz, DMSO d_6): δ 12.38 (br, s, 1H, –NH), 9.16 (br, s, 1H, –OH), 9.23 (br, s, 1H, –OH), 8.70 (s, 1H, H-2), 8.31 (s, 1H, –HC-N), 7.81 (d, $J_{(4/5)}$ = 8.2 Hz, 1H, H-4), 7.67 (d, $J_{(7/6)}$ = 8.7 Hz, 1H, H-7), 7.55–7.53 (m, 1H, H-5), 7.40–7.38 (m, 1H, H-6), 6.94 (dd, $J_{(6'/5')}$ = 7.7 Hz, $J_{(6'/4')}$ = 2.8 Hz, 1H, H-6'), 6.87 (dd, $J_{(5'/6')}$ = 7.8 Hz, $J_{(5'/4')}$ = 2.5 Hz, 1H, H-5'), 6.77 (d, $J_{(4'/5')}$ = 8.4 Hz, 1H, H-4'); ¹³C NMR (125 MHz, DMSO d_6): δ 162.3, 159.2, 155.4, 152.0, 146.4, 145.9, 125.0, 124.9, 123.8, 123.1, 122.4, 122.2, 120.2, 120.0, 119.9, 110.6, HREI-MS: m/z [M + H]⁺ calcd for C₁₆H₁₂N₂O₄ 296.0793, found 296.0787.

5.24. (*E*)-*N'*-(2-fluorobenzylidene) benzofuran-3-carbohydrazide (23)

¹H NMR (500 MHz, DMSO d_6): δ 12.45 (s, 1H, –NH), 8.98 (s, 1H, H-2), 8.29 (s, 1H, –HC-N), 8.13 (d, $J_{(6', 5')}$ = 7.2 Hz, 1H, H-6'), 8.10 (dd, $J_{(3', 4')}$ = 8.7 Hz, $J_{(3', 5')}$ = 2.2 Hz, 1H, H-3'), 7.85 (t, $J_{(4'/5', 3')}$ = 9.1 Hz, 1H, H-4'), 7.81 (d, $J_{(4/5)}$ = 7.4 Hz, 1H, H-4), 7.71–7.65 (m, 2H, H-5/H-6), 7.51 (d, $J_{(7/6)}$ = 2.2 Hz, 1H, H-7), 7.40 (t, $J_{(5'/4', 6')}$ = 9.0 Hz, 1H, H-5'); ¹³C NMR (125 MHz, DMSO d_6): δ 162.4, 159.9, 159.3, 155.5, 146.0, 132.9, 131.1, 125.0, 124.7, 123.9, 122.5, 122.3, 120.1, 118.5, 115.9, 110.7, HREI-MS: m/z [M + H]⁺ calcd for C₁₆H₁₁N₂O₂F 282.0801, found 282.0795.

5.25. (*E*)-*N'*-(4-fluorobenzylidene) benzofuran-3-carbohydrazide (24)

¹H NMR (500 MHz, DMSO d_6): δ 12.15 (s, 1H, –NH), 8.55 (s, 1H, H-2), 8.28 (s, 1H, –HC-N), 7.80 (d, $J_{(4/5)}$ = 7.4 Hz, 1H, H-4), 7.75 (d, $J_{(7, 6/ 6, 7)}$ = 6.6 Hz, 2H, H-6/H-7), 7.66–7.52 (m, 4H, H-2'/H-3'/H-5'/H-6'), 7.40–7.37 (m, 1H, H-5); ¹³C NMR (125 MHz, DMSO d_6): δ 165.5, 163.0, 159.9, 156.1, 146.6, 131.1, 131.1, 129.6, 125.6, 124.5, 123.1, 122.9, 120.7, 115.9, 115.9, 111.3; HREI-MS: m/z [M + H]⁺ calcd for C₁₆H₁₁N₂O₂F 282.0801, found 282.0795.

5.26. (*E*)-*N'*-(3-fluorobenzylidene) benzofuran-3-carbohydrazide (25)

¹H NMR (500 MHz, DMSO d_6): δ 12.02 (s, 1H, –NH), 8.89 (s, 1H, H-2), 8.31 (s, 1H, –HC-N), 7.86 (d, $J_{(4/5)}$ = 8.2 Hz, 1H, H-4), 7.80 (d, $J_{(7/6)}$ = 7.7 Hz, 1H, H-7), 7.66 (d, $J_{(6', 5')}$ = 6.6 Hz, 1H, H-6'), 7.54 (t, $J_{(2'/4', 6')}$ = 2.6 Hz, 1H, H-2'), 7.40–7.37 (m, 2H, H-5/H-6), 7.34–7.26 (m, 2H, H-4'/H-5'); ¹³C NMR (125 MHz, DMSO d_6): δ 163.3, 162.8, 159.7, 155.9, 146.4, 135.6, 130.7, 125.4, 125.2, 124.3, 122.9, 122.7, 120.5, 118.1, 114.3, 111.1; HREI-MS: m/z [M + H]⁺ calcd for C₁₆H₁₁N₂O₂F 282.0801, found 282.0795.

5.27. Assay protocol for docking study

The molecular docking study was conducted using the Molecular Operating Environment (MOE) modeling tool (Montreal, 2016) to investigate the binding manner of the synthesized compounds within the binding site of the urease enzyme. First, using MOE's built-in builder module, 3D structures for all synthesised compounds were constructed. Then, using the MOE's default parameters, all of the compounds' structures were protonated and energy was optimized. The PDB code 4ubp was used to acquire the crystal structure of the urease enzyme from the online free database RCSB. The structure was then subjected to MOE for preparation, during which all water molecules were removed, and further protonation was performed using the default parameters of MOE's structure preparation module. To obtain a stable conformation, the structure was then put through an energy minimization procedure. Finally, using MOE's default parameter, the optimized structure was employed for docking study, i.e., Placement: Triangle Matcher, Rescoring 1: London dG, Refinement: Force field, Rescoring 2: GBVI/WSA. For the ligand, a total of twenty conformations were specified prior executing the docking approach. For the protein–ligand interaction (PLI) profile, the top-ranked conformations by docking score were chosen.

5.28. Assay protocol for urease activity

The reaction mixtures, comprising 25 μ L of enzyme (jack bean urease) solution and 55 μ L of buffers containing 100 mM urea, were incubated with 5 μ L of the test compounds (0.5 mM concentration) at 30 °C for 15 min in 96-well plates. For the kinetics assessment the urea concentrations were changed from 2 to 24 mM. Urease activity was determined by measuring ammonia production using the indophenol method as described by Weatherburn. Briefly, 45 μ L of phenol reagent (1% w/v phenol and 0.005% w/v sodium nitroprusside) and, 70 μ L of alkali reagent (0.5% w/v NaOH and 0.1% active chloride NaOCl) were added to each well. The increasing absorbance at 630 nm was measured after 50 min, using a microplate reader (Molecular Device, USA). All reactions were performed in triplicate in a final volume of 200 μ L. The results (change in absorbance per min) were processed by using SoftMaxPro software (molecular Device, USA). The entire assays were performed at pH 6.8. Percentage inhibition was calculated from the formula $100 - (\text{OD}_{\text{test well}} / \text{OD}_{\text{control}}) \times 100$. Thiourea was used as the standard inhibitor for urease (Khan et al 2014).

Acknowledgment

Authors would like to thank **Institute for Research and Medical Consultations (IRMC)** at **Imam Abdulrahman Bin Faisal University (IAU)** for the laboratory facilities and for initiating the **Mawhiba Research Enrichment Program-2021** (IAU-IRMC-MAWHIBA-2021) with our long-term collaborator, “**Mawhiba**”, promoting the young talent within the kingdom.

We are highly thankful to **King Abdulaziz and His Companions Foundation for Giftedness and Creativity** for providing financial support via research agreement with IRMC, IAU.

References

- Akhtar, T., Khan, M.A., Iqbal, J., Jones, P.G., Hameed, S., 2014. A facile one-pot synthesis of 2-arylamino-5-aryloxyalkyl-1, 3, 4-oxadiazoles and their urease inhibition studies. *Chem. Biol. Drug Des.* 84 (1), 92–98.
- Alper-Hayta, S., Arisoy, M., Temiz-Arpaci, Ö., Yildiz, I., Aki, E., Özkan, S., Kaynak, F., 2008. Synthesis, antimicrobial activity, pharmacophore analysis of some new 2-(substitutedphenyl/benzyl)-5-[(2-benzofuryl) carboxamido] benzoxazoles. *Eur. J. Med. Chem.* 43 (11), 2568–2578.
- Asoh, K., Kohchi, M., Hyoudoh, I., Ohtsuka, T., Masubuchi, M., Kawasaki, K., Ebiike, H., Shiratori, Y., Fukami, T.A., Kondoh, O., 2009. Synthesis and structure–activity relationships of novel benzofuran farnesyltransferase inhibitors. *Bioorg. Med. Chem. Lett.* 19 (6), 1753–1757.
- Belluti, F., Rampa, A., Piazzini, L., Bisi, A., Gobbi, S., Bartolini, M., Andrisano, V., Cavalli, A., Recanatini, M., Valenti, P., 2005. Cholinesterase inhibitors: Xanthostigmine derivatives blocking the acetylcholinesterase-induced β -amyloid aggregation. *J. Med. Chem.* 48 (13), 4444–4456.
- Cao, J., Zhang, J., Peng, W., Chen, Z., Fan, S., Su, W., Li, K., Li, J., 2016. A Phase I study of safety and pharmacokinetics of fruquintinib, a novel selective inhibitor of vascular endothelial growth factor receptor-1,-2, and-3 tyrosine kinases in Chinese patients with advanced solid tumors. *Cancer Chemother. Pharmacol.* 78 (2), 259–269.
- Cheng, X.-S., Zhang, J.-C., You, Z.-L., Wang, X., Li, H.-H., 2014. Synthesis, structures, and Helicobacter Pylori urease inhibition of hydroxamate-coordinated oxovanadium complexes with benzohydrazone ligands. *Transition Met. Chem.* 39 (3), 291–297.
- Cowart, M., Faghhi, R., Curtis, M.P., Gfesser, G.A., Bennani, Y.L., Black, L.A., Pan, L., Marsh, K.C., Sullivan, J.P., Esbenshade, T. A., 2005. 4-(2-[2-(2-(R)-methylpyrrolidin-1-yl) ethyl] benzofuran-5-yl) benzonitrile and related 2-aminoethylbenzofuran H3 receptor antagonists potently enhance cognition and attention. *J. Med. Chem.* 48 (1), 38–55.
- Czerwonka, G., Arabski, M., Wąsik, S., Jabłońska-Wawrzycka, A., Rogala, P., Kaca, W., 2014. Morphological changes in Proteus mirabilis O18 biofilm under the influence of a urease inhibitor and a homoserine lactone derivative. *Arch. Microbiol.* 196 (3), 169–177.
- Deng, G., Xu, H., Huang, H., Jiang, J., Kun, J., Zhang, X., Li, Z., Liu, J., 2019. Synthesis and properties study of a novel nonlinear optical chromophore containing benzo [b] furan moiety based on julolidine. *J. Mol. Struct.* 1196, 439–443.
- Devesa, S.S., Blot, W.J., Fraumeni Jr, J.F., 1998. Changing patterns in the incidence of esophageal and gastric carcinoma in the United States. *Cancer: Interdisciplinary International Journal of the American Cancer Society* 83 (10), 2049–2053.
- Flynn, B.L., Gill, G.S., Grobelny, D.W., Chaplin, J.H., Paul, D., Leske, A.F., Lavranos, T.C., Chalmers, D.K., Charman, S.A., Kostewicz, E., 2011. Discovery of 7-hydroxy-6-methoxy-2-methyl-3-(3, 4, 5-trimethoxybenzoyl) benzo [b] furan (BNC105), a tubulin polymerization inhibitor with potent antiproliferative and tumor vascular disrupting properties. *J. Med. Chem.* 54 (17), 6014–6027.
- Flynn, B.L., Hamel, E., Jung, M.K., 2002. One-pot synthesis of benzo [b] furan and indole inhibitors of tubulin polymerization. *J. Med. Chem.* 45 (12), 2670–2673.
- Font, M., Domínguez, M. a.-J., Sanmartín, C., Palop, J. A., San-Francisco, S., Urrutia, O., Houdusse, F., & García-Mina, J. M. 2008. Structural characteristics of phosphoramidate derivatives as urease inhibitors. Requirements for activity. *J. Agric. Food Chem.*, 56(18), 8451-8460.
- Gfesser, G.A., Faghhi, R., Bennani, Y.L., Curtis, M.P., Esbenshade, T.A., Hancock, A.A., Cowart, M.D., 2005. Structure–activity relationships of arylbenzofuran H3 receptor antagonists. *Bioorg. Med. Chem. Lett.* 15 (10), 2559–2563.
- Habermann, J., Ley, S.V., Smits, R., 1999. Three-step synthesis of an array of substituted benzofurans using polymer-supported reagents. *J. Chem. Soc., Perkin Trans. 1* (17), 2421–2423.
- Jadhav, V., Kulkarni, M., Rasal, V., Biradar, S., Vinay, M., 2008. Synthesis and anti-inflammatory evaluation of methylene bridged benzofuranyl imidazo [2, 1-b][1, 3, 4] thiazoles. *Eur. J. Med. Chem.* 43 (8), 1721–1729.
- Karatas, F., Koca, M., Kara, H., Servi, S., 2006. Synthesis and oxidant properties of novel (5-bromobenzofuran-2-yl)(3-methyl-3-mesityl-cyclobutyl) ketonethiosemicarbazone. *Eur. J. Med. Chem.* 41 (5), 664–669.
- Khan, K.M., Naz, F., Taha, M., Khan, A., Perveen, S., Choudhary, M., Voelter, W., 2014a. Synthesis and *in vitro* urease inhibitory activity of N, N'-disubstituted thioureas. *Eur. J. Med. Chem.* 74, 314–323.
- Khan, K.M., Rahim, F., Khan, A., Shabeer, M., Hussain, S., Rehman, W., Taha, M., Khan, M., Perveen, S., Choudhary, M.I., 2014b. Synthesis and structure–activity relationship of thiobarbituric acid derivatives as potent inhibitors of urease. *Bioorg. Med. Chem.* 22 (15), 4119–4123.
- Khan, M.W., Alam, M.J., Rashid, M., Chowdhury, R., 2005. A new structural alternative in benzo [b] furans for antimicrobial activity. *Bioorg. Med. Chem.* 13 (16), 4796–4805.
- Ludden, P., Harmon, D., Huntington, G., Larson, B., Axe, D., 2000. Influence of the novel urease inhibitor N-(n-butyl) thiophosphoric triamide on ruminant nitrogen metabolism: II. Ruminant nitrogen metabolism, diet digestibility, and nitrogen balance in lambs. *J. Anim. Sci.* 78 (1), 188–198.
- Luo, W., Yu, Q.-S., Zhan, M., Parrish, D., Deschamps, J.R., Kulkarni, S.S., Holloway, H.W., Alley, G.M., Lahiri, D.K., Brossi, A., 2005. Novel anticholinesterases based on the molecular skeletons of furobenzofuran and methanobenzodioxepine. *J. Med. Chem.* 48 (4), 986–994.
- Mahboobi, S., Uecker, A., Cénac, C., Sellmer, A., Eichhorn, E., Elz, S., Böhmer, F.-D., Dove, S., 2007. Inhibition of FLT3 and PDGFR tyrosine kinase activity by bis (benzo [b] furan-2-yl) methanones. *Bioorg. Med. Chem.* 15 (5), 2187–2197.
- Martelli, A., Buli, P., Cortecchia, V., 1981. Urease inhibitor therapy in infected renal stones *Advances in Nephrology*. Springer, pp. 431–439.
- Milyutin, C.V., Lichitsky, B.V., Melekhina, V.G., Komogortsev, A.N., Fakhruddinov, A.N., Minyaev, M.E., Krayushkin, M.M., 2020. Synthesis of 1H-pyrano [4, 3-b] benzofuran-1-one derivatives via photochemical cyclization of substituted 4H-furo [3, 2-c] pyran-4-ones. *Tetrahedron Lett.* 61, (44) 152469.
- Mobley, H., Hausinger, R., 1989. Microbial ureases: significance, regulation, and molecular characterization. *Microbiol. Rev.* 53 (1), 85–108.
- Montreal, C.C.G.I., 2016. Molecular operating environment (MOE): Chemical Computing Group Inc. 1010 Sherbooke St. West, Suite# 910, Montreal . . .
- Oter, O., Ertekin, K., Kirilmis, C., Koca, M., Ahmedzade, M., 2007. Characterization of a newly synthesized fluorescent benzofuran derivative and usage as a selective fiber optic sensor for Fe (III). *Sensors Actuators B: Chem.* 122 (2), 450–456.
- Peschke, B., Bak, S., Hohlweg, R., Nielsen, R., Viuff, D., Rimvall, K., 2006. Benzo [b] thiophene-2-carboxamides and benzo [b] furan-2-carboxamides are potent antagonists of the human H3-receptor. *Bioorg. Med. Chem. Lett.* 16 (12), 3162–3165.
- Rollas, S., Küçükgüzel, S.G., 2007. Biological activities of hydrazone derivatives. *Molecules* 12 (8), 1910–1939.
- Narang, R., Narasimhan, B., Sharma, S., 2012. A review on biological activities and chemical synthesis of hydrazide derivatives. *Cur. Med. Chem.* 19 (4), 569–612.
- Negi, V.J., Sharma, A.K., Negi, J.S., Ra, V., 2012. Biological activities of hydrazone derivatives in the new millennium. *Int. J. Pharm. Chem.* 4, 100–109.

- Rahim, F., Zaman, K., Ullah, H., Taha, M., Wadood, A., Javed, M. T., Rehman, W., Ashraf, M., Uddin, R., Uddin, I., 2015. Synthesis of 4-thiazolidinone analogs as potent in vitro anti-urease agents. *Bioorg. Chem.* 63, 123–131.
- Romagnoli, R., Baraldi, P.G., Sarkar, T., Carrion, M.D., Cruz-Lopez, O., Cara, C.L., Tolomeo, M., Grimaudo, S., Di Cristina, A., Pipitone, M.R., 2008. Synthesis and biological evaluation of 2-(3', 4', 5'-trimethoxybenzoyl)-3-N, N-dimethylamino benzo [b] furan derivatives as inhibitors of tubulin polymerization. *Biorg. Med. Chem.* 16 (18), 8419–8426.
- Saeed, A., Khan, M.S., Rafique, H., Shahid, M., Iqbal, J., 2014. Design, synthesis, molecular docking studies and in vitro screening of ethyl 4-(3-benzoylthioureido) benzoates as urease inhibitors. *Bioorg. Chem.* 52, 1–7.
- Saify, Z.S., Kamil, A., Akhtar, S., Taha, M., Khan, A., Khan, K.M., Jahan, S., Rahim, F., Perveen, S., Choudhary, M.I., 2014. 2-(2'-Pyridyl) benzimidazole derivatives and their urease inhibitory activity. *Med. Chem. Res.* 23 (10), 4447–4454.
- Sravanthi, K., Khan, F.A., 2020. Brønsted acid-induced synthesis of methyl benzofurans via Grob type fragmentation of norbornyl derivatives. *Tetrahedron Lett.* 61, (38) 152351.
- Taha, M., Ismail, N.H., Baharudin, M.S., Lalani, S., Mehboob, S., Khan, K.M., Siddiqui, S., Rahim, F., Choudhary, M.I., 2015. Synthesis crystal structure of 2-methoxybenzoylhydrazones and evaluation of their α -glucosidase and urease inhibition potential. *Med. Chem. Res.* 24 (3), 1310–1324.
- Taha, M., Rahim, F., Ullah, H., Wadood, A., Farooq, R.K., Shah, S. A.A., Nawaz, M., Zakaria, Z.A., 2020. Synthesis, in vitro urease inhibitory potential and molecular docking study of benzofuran-based-thiazolidinone analogues. *Sci. Rep.* 10 (1), 1–8.
- Weatherburn, M., 1967. Phenol-hypochlorite reaction for determination of ammonia. *Anal. Chem.* 39 (8), 971–974.